

SWMManywhere: A Global-scale Workflow for Generation and Sensitivity Analysis of Synthetic Urban Drainage Models

Barnaby Dobson¹, Tijana Jovanovic², Diego Alonso-Álvarez³, Taher Chegini⁴

¹Department of Civil Engineering, Imperial College London, UK

²British Geological Survey, UK

³Department of Computing, Imperial College London, UK

⁴Purdue University, USA

Statement

The submitted version on EarthArXiv is a non-peer reviewed preprint. This manuscript has, however, been submitted for peer review in the Journal of Hydrology. Subsequent versions of this manuscript may have slightly different content. If accepted, the final version of this manuscript will be available via the 'Peer-reviewed Publication DOI' link on the right-hand side of this webpage.

16 **Highlights**

- 17 - SWMMAnywhere can synthesise an urban drainage network model anywhere in the
18 world
- 19 - SWMMAnywhere is a parameterised approach for customising the synthesised
20 network
- 21 - We use sensitivity analysis to investigate uncertainty of network synthesis
- 22 - We find significant interaction between parameters, suggesting an ensemble
23 approach
- 24 - Parameters controlling surface observable network elements are most sensitive

25 **Abstract**

26 Continual improvements in publicly available global geospatial datasets provide an
27 opportunity for deriving urban drainage networks and simulation models of these networks
28 (UDMs) worldwide. We present SWMMAnywhere, which leverages such datasets for
29 generating synthetic UDMs and creating a Storm Water Management Model for any urban
30 area globally. SWMMAnywhere's highly modular and parameterised approach enables
31 significant customisation to explore hydraulically feasible network configurations. Key novelties
32 of our workflow are in network topology derivation that accounts for combined effects of
33 impervious area and pipe slope. We assess SWMMAnywhere by comparing pluvial flooding,
34 drainage network outflows, and design with known networks. The results demonstrate high
35 quality simulations are achievable with a synthetic approach even for large networks. Our
36 extensive sensitivity analysis shows that the locations of manholes, outfalls, and underlying
37 street network are the most sensitive parameters. We find widespread sensitivity across all
38 parameters without clearly defined values that they should take, thus, recommending an
39 uncertainty driven approach to synthetic drainage network modelling. This study showcases
40 significant potential of SWMMAnywhere for research and industry applications to provide
41 drainage network models in urban areas where traditional approaches are impractical.

42 **1 Introduction**

43 Urban drainage models (UDMs) are representations of land and pipes that can be simulated
44 with hydraulic models such as Storm Water Management Model (SWMM) (Rossman, 2010).
45 UDMs are essential for managing stormwater, preventing flooding, and ensuring the
46 sustainability of urban water systems (Butler and Davies, 2004). UDM simulations capture
47 the behaviour of drainage networks under various rainfall scenarios, enabling planners to
48 design effective infrastructure and mitigate risks (Bach et al., 2014). However, the
49 development of UDMs typically requires extensive infrastructure records on the connectivity,
50 geometric properties, and elevations of underground pipes (Bach et al., 2020; Chahinian et
51 al., 2019). In cases where these records are unavailable, whether due to ownership issues
52 or simply that they do not exist, the expense of creating a UDM becomes significant because
53 of costly surveying requirements. To forgo this expense, it may be preferable to synthesise
54 a UDM based on the underlying information governing the placement and sizing of drainage
55 pipes, most generally, surface elevation, building locations, and road locations (Chegini and
56 Li, 2022).

57 The earliest methods to create synthetic UDM exploited the fractal nature of a drainage
58 network and, while simulations were not tested, demonstrated that the broad statistical
59 properties of the network, i.e., distribution of flow path lengths, could be estimated (Ghosh et
60 al., 2006). When road network and elevation data were incorporated, the accuracy of
61 synthesised UDMs improved and simulations approached those of a real UDM for the same
62 locale (Blumensaat et al., 2012). Generally, UDM synthesis involves three main tasks:
63 delineating surface characteristics, deriving network topology, and hydraulic design, each of
64 which will be reviewed below.

65 First, surface characteristics, hereafter referred to as sub-catchments, quantify the spatial
66 distribution of stormwater drainage from impervious areas to manholes. Sub-catchment
67 delineation has received the least attention in UDM synthesis literature and most commonly
68 follows a watershed delineation approach (Blumensaat et al., 2012; Warsta et al., 2017). The

69 drained impervious area within a delineated sub-catchment is typically calculated from the
70 area covered by roads and buildings (Mair et al., 2017; Chegini and Li, 2022). However,
71 another simpler method is to assign impervious areas to drain to a nearest manhole (Reyes-
72 Silva et al., 2023). Both methods require identification of manholes, highlighted as critical
73 future work in Blumensaat et al., (2012), but has received little attention since (Bertsch et al.,
74 2017; Chahinian et al., 2019). We place sub-catchment delineation and manhole
75 identification as the first tasks to perform during UDM synthesis, since network topology and
76 hydraulic design should account for the impervious area contributing to a given pipe.

77 Second, network topology describes the spatial layout of a UDM, connectivity of pipes, and
78 connectivity of the sub-catchments to UDM, i.e., through manholes. Network topology is
79 typically derived by asserting that pipes follow roads, thus dramatically reducing the
80 dimensionality of deriving network topology (Mair et al., 2017; Xu et al., 2021). An efficient
81 network that visits all manholes without redundant pipes can be derived using a shortest
82 path-based algorithm. This algorithm minimizes the total graph cost, with each edge (i.e., a
83 plausible pipe) assigned an individual cost that represents some penalty associated with
84 retaining that edge. Chahinian et al. (2019) provide a detailed exploration minimising costs
85 based on pipe length, pipe adjacent angle, and slope, and highlighting the importance of
86 slope as a cost. Reyes-Silva et al. (2023) derive the UDM by applying the minimum
87 spanning tree (MST) to a full street network to minimise the number of pipes. This approach,
88 however, does not inherently consider slope in the deriving network topology step since MST
89 is only applicable to undirected networks, instead gravitational slope along pipes is enforced
90 as a postprocessing correction. A minimum spanning arborescence is an alternative
91 approach to solve such a problem for a directed network (Ray and Sen, 2024; Tarjan, 1977),
92 although has not yet been demonstrated in UDM synthesis. Furthermore, an additional cost
93 to be minimised that has not been tested in the literature is the need to minimise the
94 impervious contributing area to a given pipe and thus more evenly distribute flow throughout

95 the network, much in the manner of the original proposed fractals for network topology
96 (Ghosh et al., 2006).

97 Third, hydraulic design refers to the selection of pipe diameter, invert levels, and other pipe
98 hydraulic parameters in a synthetic UDM, which typically follows local standards (Chegini
99 and Li, 2022; Duque et al., 2022; Reyes-Silva et al., 2023). Duque et al. (2022), present a
100 methodology for designing sanitary sewer networks by starting from the most upstream
101 pipes, iteratively working downstream, and designing each pipe by minimising the costs
102 subject to the feasibility of design constraints; such an approach could be equally valid for a
103 UDM. In cases where the impervious contributing area of a given pipe has been
104 synthesised, a Rational Method could be applied for determining pipe size. A variety of more
105 extensive global optimisation methods exist for hydraulic design to both minimise costs (e.g.,
106 Sun et al., (2011)), or calibrate to observations (e.g., Huang et al., (2022); Sytsma et al.,
107 (2022)). However, these calibration studies highlight the inherent equifinality in parameter
108 selection, thus suggesting the uncertainties in such a high dimensionality problem may
109 outweigh any 'optimal' algorithm.

110 Because UDM synthesis requires a hydraulic design, equifinality must also be inherent to
111 UDM synthesis. We argue that this has been under-recognised in existing UDM synthesis,
112 primarily because of a lack of data and the absence of an automated, end-to-end workflow to
113 assess the impact of parameter selection. A reader may observe results from the
114 supplement of Duque et al., (2022), which demonstrates that small changes in their grid
115 scale for the synthesis algorithm can generate dramatically different sanitary sewer
116 networks.

117 An equally valid line of inquiry is, therefore, to examine UDM synthesis with sensitivity
118 analysis to quantify the importance of various factors in generating more realistic networks
119 (Pianosi et al., (2016)). Sensitivity analysis provides verification by revealing ranges of
120 'behavioural' parameter values that produce acceptable model outputs, thus informing
121 application of UDM synthesis in data-sparse regions. Additionally, it reveals the dominant

122 controls and key processes governing UDM synthesis by quantifying the relative importance
123 of different parameters. In turn, revealing where uncertainty reduction may be most
124 beneficial. We do not assume that accurate UDM synthesis is possible in every location
125 using solely building, road, and elevation data, particularly given the complexities involved in
126 the gradual expansion of a UDM (Rauch et al., 2017). However, it is impractical to improve
127 UDM synthesis by capturing every possible element involved in network evolution. Instead,
128 sensitivity analysis provides an objective way to guide improvement; prioritising
129 measurements and processes that relate to the most sensitive parameters.

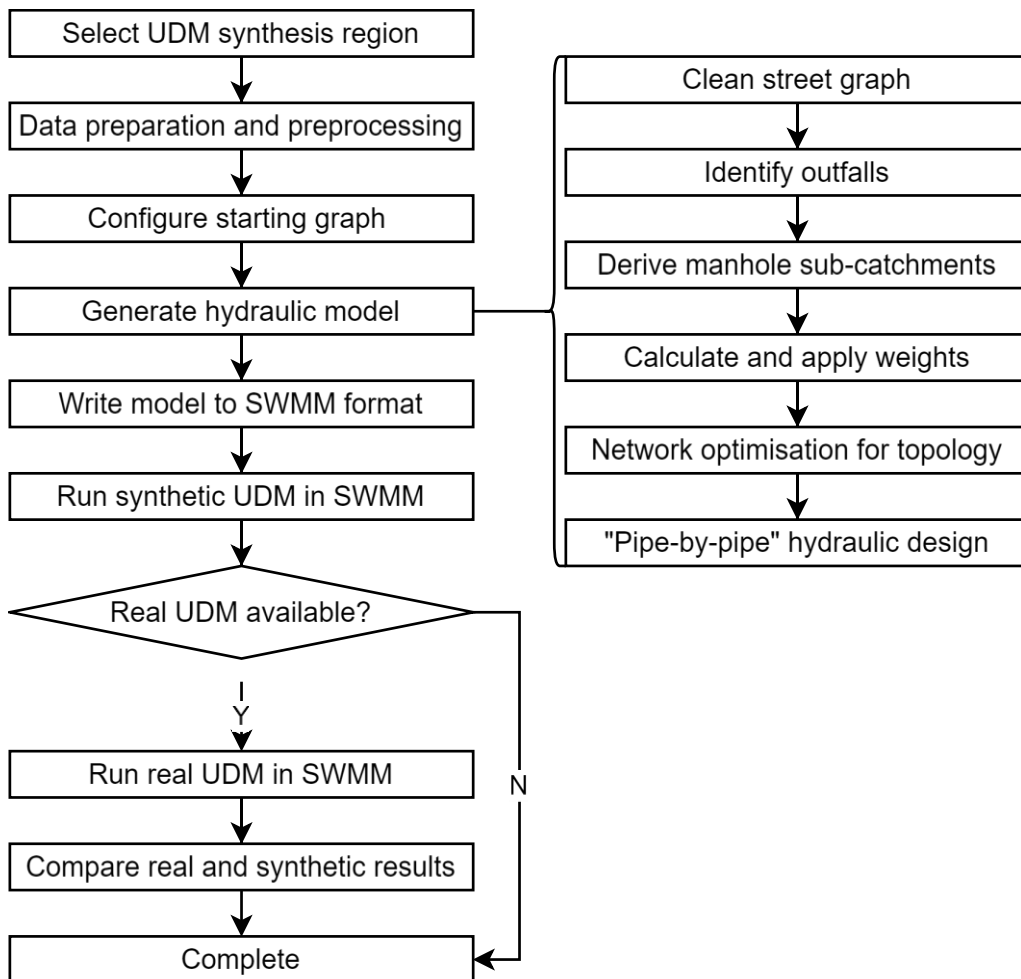
130 Continual improvements in development and accessibility of remote sensing and open
131 geospatial data at global scale facilitates applicability of UDM synthesis in many locations.
132 Chegini et al., (2022), demonstrate an approach that can perform network topology and the
133 dimensioning part of hydraulic design anywhere in the continental United States. Montalvo et
134 al., (2024) implement the UDM synthesis algorithm presented by Reyes-Silva et al., (2023),
135 in a GIS tool, however this approach does not acquire/process the necessary geospatial
136 data nor is it open-source at time of writing. We believe that a global tool, that is open-
137 source, and tailored to accommodate the uncertainty inherent in the UDM synthesis problem
138 would be of great value to the urban drainage community. Such a tool would enable
139 hydrodynamic method developers to bypass the reproducibility crisis (Stagge et al., 2019;
140 Hutton et al., 2016), by demonstrating their tools on an unlimited suite of UDMs synthesised
141 in cities worldwide, improving on the entirely theoretical test suites that presently exist
142 (Möderl et al., 2011, 2009; Sweetapple et al., 2018). Furthermore, it would contribute
143 towards better representation of urban environments in the regional hydrological cycle,
144 which is a critical and under-represented component of such applications (Coxon et al.,
145 2024).

146 In this paper we present a workflow, called SWMManywhere, to synthesise UDMs anywhere
147 in the world. We show its versatility by applying it to multiple case studies (i.e. sewer
148 systems of different sizes in two different countries) and to facilitate its global usage we

149 deploy it as an open-source Python tool (Dobson et al., 2024a) with extensive
 150 documentation (SWMMAnywhere documentation, 2024). SWMMAnywhere provides a
 151 parameterised and easy to customise approach for UDM synthesis which allows us to
 152 perform sensitivity analysis of synthesised UDMs. We ensure SWMMAnywhere responds to
 153 the need for worldwide application by using open global datasets and including the retrieval
 154 and preprocessing of these datasets as part of the algorithm. The methods implemented in
 155 SWMMAnywhere also include a variety of technical novelties in the field of UDM synthesis,
 156 including use of a minimum spanning arborescence to derive topology, enabling
 157 minimisation of contributing area during this process, and implementing Duque et al.,
 158 (2022)'s pipe-by-pipe design method for urban drainage networks.

159 2 Methodology

160 A high-level overview of our proposed SWMMAnywhere workflow is shown in Figure 1.



161

162 *Figure 1: Overview of the SWMManywhere workflow.*

163 We present an end-to-end workflow for UDM synthesis and comparison against a real UDM,
164 if available, anywhere in the world. A key barrier to UDM synthesis identified in literature is
165 difficulty in setting up a hydraulically correct model, thus we specify data acquisition and
166 preprocessing in the workflow. The 'generate hydraulic model' step, is the key step that
167 should ultimately create sub-catchments, a network topology, and hydraulic designs of pipes
168 that together fully describe the synthesised drainage network. Such a drainage network, i.e.,
169 the synthetic UDM, will be valid for simulation in a widely used software for design and
170 analysis of drainage networks, such as SWMM, enabling studying different precipitation
171 events and inspecting state variables such as pipe flows and pluvial flooding. In Section 2.1,
172 we describe the theory and processes in our workflow, also explaining how it can be
173 customised with parameter choices and additional processes to vary the nature of the
174 synthesised UDM.

175 A key hypothesis that must underlie any synthetic UDM approach is that results may be valid
176 in places where a real UDM is not available or not trusted. Because we observed the
177 sensitivity to parameter selection in previous UDM synthesis literature, we intentionally
178 specify SWMManywhere to be highly parameterised and customisable. We use sensitivity
179 analysis on these parameters to demonstrate how they impact synthesised networks. In
180 Section 2.2, we describe how sensitivity analysis can guide the use of SWMManywhere in
181 areas where parameters cannot be estimated a priori based on field data and provide a
182 deeper understanding of UDM synthesis. We apply this analysis to eight UDMs in two
183 different locations.

184 We discuss UDM synthesis using graph theory terminology:

- 185 • A graph represents the UDM, consisting of nodes (manholes) that are connected by
186 edges (pipes). The graph can be either undirected or directed, indicating that
187 connections are between two nodes (undirected) or from one node to another
188 (directed). Pipes are undirected since head may drive uphill flow, however, treating

189 the graph as directed enables better description of preferential flow paths and is also
190 the format required by SWMM, SWMMAnywhere makes use of both directed and
191 undirected graphs.

- 192 • In graph theory, a subgraph refers to a sub-selection of the graph and is called a
193 connected component if every node is in the subgraph reachable from every other
194 node within that subgraph. Connected components are used in SWMMAnywhere to
195 describe a collection of manholes and pipes that drain to a common outfall.
- 196 • The topology of the graph captures the overall arrangement and relationships of
197 nodes and edges and can be thought of as the pipe layout in a UDM. The edges can
198 have costs, for example length, which may be minimised by shortest path algorithms
199 to minimise flow routes. Flow routes should be minimised in any drainage network to
200 drain the catchment as efficiently as possible, preventing the accumulation of water
201 and flooding of manholes. A minimum spanning tree is a subgraph that connects all
202 nodes with the minimum possible total edge cost for an undirected graph, a minimum
203 spanning arborescence is the same for a directed graph, thus these represent the
204 most cost-efficient pipe layouts that may exist for a given area. We will refer to a
205 graph of potential pipe-carrying edges as the street graph, while the optimised layout
206 is the UDM topology.

207 2.1 SWMMAnywhere

208 2.1.1 *Data and preparation*

209 Our SWMMAnywhere approach uses datasets that are of sufficient level of detail to be used
210 in global application: road locations, river locations, elevation, and building footprints. We
211 stress that these datasets, in particular road locations and building footprints, vary in quality
212 from location to location, thus, the downloaded data for a given case study should always be
213 inspected carefully. Additionally, we enable manually sourced, higher quality data for input, if
214 available, as described in the online documentation (SWMMAnywhere documentation,

215 2024). The default datasets are visualised for one of our case studies in Figure 2, and
216 described in further detail in this section.



217

218 *Figure 2: Visualisation of downloaded data in the Cran Brook, UK. See main text for citations.*

219 *Streets and rivers*

220 Assuming pipes can only exist in pre-specified plausible locations will dramatically reduce
221 the dimensionality of the shortest-path UDM topology derivation. Thus, we assume that
222 pipes can only exist in certain locations, typically streets due to the common validity of this
223 assumption (Mair et al., 2017). In addition, paved streets constitute one of the key
224 impervious surfaces which must be drained in a UDM. Rivers are also downloaded as these
225 are potential outfall locations of the drainage network, described in further detail in Section

226 2.1.2. OpenStreetMap (OSM) provides street and river data worldwide and is used in this
227 study.

228 *Impervious areas*

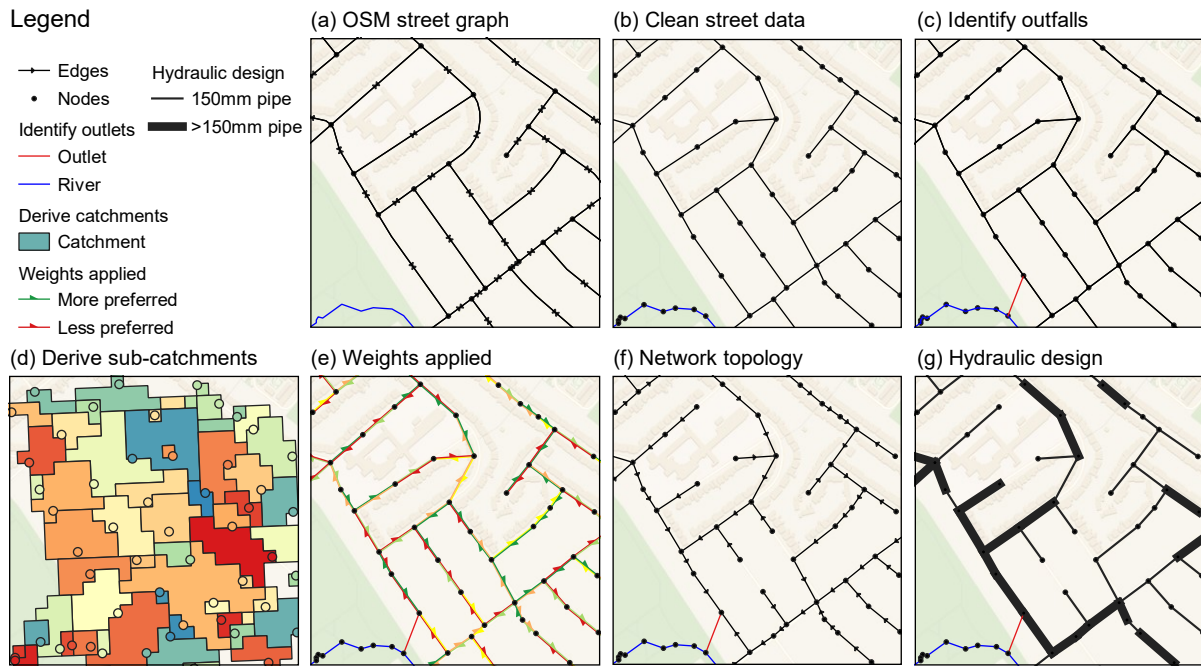
229 To calculate the impervious area of a sub-catchment, and thus enable runoff generation, we
230 use road locations, their number of lanes, which are contained within OSM, and building
231 footprints. Recent advances in machine learning have enabled identification of building
232 perimeters from high-resolution satellite data worldwide. Two large datasets, provided by
233 Google and by Microsoft, are now combined and available at (Google-Microsoft Open
234 Buildings, 2024). Both datasets use convolutional neural networks to classify pixels as
235 buildings (Tan and Le, 2019; Sirko et al., 2021) and custom methods to polygonise these
236 pixels into buildings (Sirko et al., 2021; Computer generated building footprints for the United
237 States, 2024). The authors would note that, although global, this dataset has varying quality
238 in different regions due to the nature of the training data that was used and resolution of
239 satellite imagery. Although other impervious surfaces besides roads and buildings, such as
240 car parks, that must be drained in a UDM are common, we could not identify global datasets
241 describing these, and thus consider them currently outside the scope of this study.

242 *Elevation*

243 Elevation data, in the format of a Digital Elevation Model (DEM), is essential to delineate
244 manhole sub-catchments, to calculate the slope along edges, and to identify if there are
245 paths in the street graph that should not be ignored, for example, those at that span different
246 hydrological catchments. We use NASADEM, which is a publicly available radar-based
247 global DEM at 30m resolution (Crippen et al., 2016), from Microsoft Planetary Computer
248 (Source et al., 2022). Although higher resolutions around 2m are recommended for UDM
249 (Arrighi and Campo, 2019), such datasets do not yet exist openly at global scales.

250 2.1.2 Pipe network generation

251 A key innovation of our approach is to iteratively process a street graph and gradually
252 transform it into a UDM with full hydraulic design. These processes must take a graph and
253 return a graph. The key tasks that they perform are summarised in Figure 3, discussed
254 further in this section and used for the experiments in this paper.



255

256 *Figure 3: Visualisation of key iterations to the graph as different processes are applied. Catchments (D) are*
257 *coloured by the manhole that they drain to.*

258 Table 1 lists all tuneable parameters of our proposed workflow, with reasonable default
259 values for these parameters and their ranges provided in the online documentation
260 (SWMManywhere documentation, 2024). We carry out an extensive sensitivity analysis (see
261 Section 2.2) to identify any behavioural ranges of these parameters and identify their relative
262 importance in UDM synthesis.

263
264
265

Table 1: SWMManywhere user adjustable parameters that are tested in sensitivity analysis for this work, a full list of parameters is available in the online documentation (SWMManywhere documentation, 2024). If the variable is described differently from its use in the software to improve clarity, the software term is indicated in brackets.

GROUP	VARIABLE	KEY
SYSTEM DESCRIPTION (MANHOLES AND OUTFALLS)	node merge distance	pNM
	outfall length	pOL
	max street length	pXS
	river buffer distance	pRB
TOPOLOGY DERIVATION	chahinian slope scaling	pSS
	chahinian angle scaling	pAS
	length scaling	pLS
	contributing area scaling	pCS
	chahinian slope exponent	pSE
	chahinian angle exponent	pAE
	length exponent	pLE
	contributing area exponent	pCE
HYDRAULIC DESIGN	max filling ratio (max fr)	pFR
	min v	pMV
	max v	pXV
	min depth	pMD
	max depth	pXD
	design precipitation (precipitation)	pDP

266

267 *Data cleaning and manhole identification*

268 As explained in Section 2.1.1, OpenStreetMap (OSM) is the default data source for obtaining
 269 street and river graphs. However, the raw OSM data are not directly suitable for UDM
 270 generation, so we perform a variety of data cleaning operations to create a more suitable
 271 graph for UDM synthesis, as illustrated in Figure 3a-b. The first significant process in data
 272 cleaning is enforcing a maximum edge length, splitting edges that are longer than max street
 273 length parameter (*pXS*, Table 1). The second is merging of nodes, which joins nodes
 274 together if they are within a specified distance of each other (*node merge distance*, *pNM*).
 275 These two processes jointly control where manholes are located along edges and the
 276 frequency with which they occur. The final significant task in data cleaning is buffering street
 277 paths in proportion to the number of lanes to create a shapefile of impervious street area.
 278 The remainder of processing in this stage is perfunctory, performing tasks such as ensuring
 279 consistent geometries, a consistent identification scheme, removing parallel edges, and

280 converting the directed street graph to an undirected graph (as a pipe may flow in a direction
281 opposite to road travel).

282 *Sub-catchment outline and surface characteristics*

283 We begin the sub-catchment delineation, by first burning the road network into the DEM of
284 an urban area. This burning process is a common practice in UDM sub-catchment
285 representation (Gironás et al., 2010) and involves lowering the elevation of grid cells in the
286 DEM that contain roads. Then, we hydrologically condition the DEM by breaching
287 depressions (Lindsay, 2016a). Upon conditioning the DEM, we compute the flow direction,
288 using the D8 method (O'Callaghan and Mark, 1984), and slope. Because our workflow
289 includes generation of a SWMM model, a sub-catchment width parameter is required. We
290 follow the approach proposed by InfoWorks (Subcatchment Data Fields (InfoWorks), 2024)
291 to compute the width of a sub-catchment based on the radius of a circle with area equal to
292 the area of the sub-catchment.

293 *Outfall identification*

294 Another key feature of a UDM is outfall locations. The first step in identifying outfalls requires
295 assessing the topology of the graph to ensure its hydrologic feasibility (Seo and Schmidt,
296 2013; Li and Willems, 2020). To achieve this, we remove edges that cross the boundaries of
297 hydrological catchments (defined as the largest non-overlapping drainage basins in the
298 study region), because these are unlikely to carry a pipe. Then, we identify potential outfall
299 locations by assuming that outfalls may only exist within a specified distance of a river (*river*
300 *buffer distance, pRB*). Although other factors such as environmental considerations affect
301 selection of the outfall location, in this study, we only account for the vicinity of water bodies.
302 We incorporate the relative construction cost of outfalls in our workflow, by assigning weights
303 to the identified outfall locations based the length of the pipe that connects the network to
304 the river (*outfall length, pOL*). If no potential outfalls are identified the node with the lowest
305 elevation is used as the outfall. On the other hand, in cases where multiple plausible outfalls

306 are identified, we retain them all at this step and determine the outfall during the network
307 topology derivation step.

308 *Calculating weights and network topology*

309 The network topology can be derived as a minimisation problem of overall graph cost. This
310 minimisation should start with a graph of potential edges (i.e., the graph up to this point) and
311 return a directed graph that visits all nodes (manholes), minimising overall graph cost,
312 without retaining redundant edges (pipes), which is also referred to as a minimum spanning
313 arborescence (MSA).

314 The first step to take in network topology derivation is to identify how each edge contributes
315 to the overall graph cost. As identified by Chahinian et al., (2019), it is plausible that each of
316 pipe length, pipe slope and pipe adjacent angle (the angle at which two joining pipes meet)
317 are important to consider for minimisation. We further propose that the total contributing area
318 carried by pipes in the derived network should also be minimised. As with *ibid.*, these factors
319 do not necessarily contribute to the overall graph cost symmetrically or proportionally. For
320 example, while both negative slopes and overly steep positive slopes are penalised, the
321 penalisation on negative slopes increases with slope more sharply than for positive slopes,
322 because the former becomes hydraulically impractical more quickly than the latter. It is not
323 apparent which of these factors (slope, angle, area, and length) are more important to
324 minimise than others and so we combine each factor to be varied, as in *ibid.* We deviate
325 from *ibid.* by assigning both a linear and exponential scaling parameter to each factor (rather
326 than solely linear), enabling high customisation of how overall graph cost is calculated (i.e.,
327 parameters in the *topology derivation* group). We calculate each individual factor, apply
328 scaling parameters, and sum these into an overall cost for each edge in the graph,
329 producing a graph such as that visualised in Figure 3e.

330 The network topology is then derived using an implementation based on the shortest-path
331 algorithm proposed by Tarjan (1977), to find the MSA of the graph. The algorithm starts from

332 a designated "waste" node that all potential outfall locations are connected to, either directly
333 or through river paths, thus enabling all connected component subgraphs to be handled in a
334 single pass. The algorithm initializes a priority queue with the waste node's incoming edges,
335 sorted by their costs. At each step, the minimum cost edge is extracted from the priority
336 queue. If the node it leads to is not already included in the arborescence being constructed,
337 that node and edge are added to the arborescence. The node is marked with its parent, and
338 any edges incoming to that node are added to the priority queue. This process continues
339 until all nodes are included in the arborescence. The final arborescence represents the UDM
340 network topology, where the selected edges correspond to the pipe segments that must be
341 hydraulically designed.

342 *Hydraulic design*

343 Duque et al., (2022), propose a "pipe-by-pipe" method to design sanitary sewer network
344 pipes, the method starts at the most upstream pipes, designing each pipe in terms of
345 diameter and depth under a set of design constraints (see *hydraulic design* group), and
346 continues iterating downstream. They demonstrate that this method is comparable to an
347 optimal dynamic programming-based approach, although is significantly more efficient. We
348 adapt the pipe-by-pipe approach to make it suitable for a SWMManywhere approach:

- 349 • Rather than deriving the design flow from household waste generation, we use a
350 Rational method that calculates the design flow as the entire impervious area in sub-
351 catchments upstream of the pipe being designed multiplied by a *design precipitation*,
352 *pDP*, amount.
- 353 • Inspection of any large real UDM will commonly reveal pipes travelling in an uphill
354 direction, as measured by surface elevation. Wherever possible the pipe's elevation
355 will be such that they flow downhill despite the surface elevation, however there is no
356 guarantee that any hydraulically feasible design will exist. Because Duque et al.
357 (2022) derive network topology using hydrological flow paths a feasible design will
358 always exist, however this is not the case for SWMManywhere, which uses streets

359 for pipe locations and accounts for factors besides slope during network topology
360 derivation. To accommodate this, we include a surcharge feasibility constraint, which
361 allows a pipe to be designed for flow under surcharge, provided this is the only way
362 to reach a feasible hydraulic design.

- 363 • To provide better performance, we assess all designs for a pipe rather than selecting
364 the first feasible design. The selected design first aims to satisfy feasibility
365 constraints, and if no feasible design exists, picking the most feasible design. It then
366 minimises depth, diameter, and excavation cost, as calculated in Duque et al. (2022).

367 The final product is a fully described UDM, complete with sub-catchments and hydraulic
368 designs, thus sufficient to be simulated in software such as SWMM.

369 *2.1.3 Measuring effectiveness of UDM synthesis*

370 The question of ‘how realistic is a synthesised UDM’ is most sensibly assessed by
371 comparing synthesised results against a real UDM. UDM synthesis in a sensitivity analysis
372 context requires understanding why we see the results that we see. Thus, an extensive suite
373 of allowable performance metrics is provided covering a variety of different measures and
374 variables, see Table 2 for a list of the metrics used in this study. We define metrics that
375 measure performance for different elements of UDM synthesis. System description metrics
376 assess the synthesised UDM in terms of properties that describe infrastructure, topology
377 metrics investigate the layout of the graph, and design metrics assess the derived diameter
378 of pipes. Furthermore, the UDM is simulated in SWMM and thus simulated flow, and flooding
379 can also be compared.

380 *Table 2: List of metrics implemented in SWMManywhere*

CATEGORY	MEASURE	VARIABLE	KEY
SYSTEM DESCRIPTION	reerror	length	mRL
	reerror	npipes	mRP
	reerror	nmanholes	mRM
TOPOLOGY	deltacon0	-	mD0
	laplacian distance	-	mLD
	vertex edge distance	-	mVD
	kstest	edge betweenness	mKE
	kstest	node betweenness	mKN
DESIGN	reerror	diameter	mRD
	kstest	diameter	mKD
SIMULATION	nse	flow	mNQ
	kge	flow	mKQ
	reerror	flow	mRQ
	nse	flooding	mNF
	kge	flooding	mKF
	reerror	flooding	mRF

381 Comparing flow and/or flooding simulations is typical in the UDM synthesis literature (Reyes-
382 Silva et al., 2023; Blumensaat et al., 2012). We create a timeseries of total flooded volume to
383 assess flooding simulation performance across the entire network. Meanwhile, flows are
384 assessed at the system outfall, as with (Blumensaat et al., 2012). However, unlike existing
385 literature, which assumes that the outfall locations of the network being synthesised are
386 known, we do not make this assumption, as this information is not globally available.

387 Instead, we identify where synthetic manholes fall inside sub-catchments of the real network.
388 From these classified manholes it identifies the most commonly represented outfall, and sub-
389 selects only that connected component for comparison purposes.

390 Because the reasons for performing sensitivity analysis are to understand how parameters
391 change behaviours in UDM synthesis, the most common measure of performance we use is

392 the relative error (*relerror* measure in Table 2, equation 1), which is simple to understand
393 and provides directionality in terms of over/under estimation,

$$relerror = \frac{mean(synthetic) - mean(real)}{mean(real)} \quad (1),$$

394 where *synthetic* is the synthetic UDM data to be compared against the *real* data. We omit a
395 conventional *time* component of the metric because the same equation can equally be used
396 for timeseries or design properties (such as average diameter) alike. In cases of comparing
397 flow or flooding timeseries, we also include the Nash-Sutcliffe Efficiency and Kling-Gupta
398 Efficiency, because these are commonly used and so will provide users who are familiar with
399 them a more nuanced grasp of the synthetic UDM's performance.

400 A further set of measures that can be used for synthetic networks are those that test the
401 topological similarity of the derived vs real network, we implement a variety of those
402 presented in existing literature (Wills and Meyer, 2020; Chegini and Li, 2022), see *topology*
403 category in Table 2.

404 2.1.4 Implementation

405 SWMManywhere is a highly modular workflow and in this study, we implement it in Python
406 and publish it as an open-source tool (Dobson et al., 2024a). We note that the workflow is
407 general and can be implemented in any other programming language. In our implementation
408 of SWMManywhere the minimal required user input is the bounding box of the target urban
409 area, and all remaining steps Figure 1 are automated. The bounding box should be provided
410 in terms of latitudes and longitudes in WGS 84 geographic coordinate system (EPSG:4326).
411 SWMManywhere will reproject all downloaded data into the Universal Transverse Mercator
412 (UTM) coordinate system. UTM uses a coordinate system with metre as its unit, and thus
413 can provide accurate distance and area calculations in contrast to WGS 84. The UTM is split

414 into zones and the zone ultimately used in a SWMManywhere run is calculated based on the
415 UTM zone of the bounding box.

416 As we described in Section 2.1.2 the most complex step in the workflow is the pipe network
417 generation, i.e., iteratively applying various graph operations to the initial graph street to
418 generate the final UDM. These operations, referred to in our implementation as graph
419 functions, have a variety of parameters that need to be specified, as listed in Table 1.
420 Considering the importance of graph functions and to accommodate flexibility in applying
421 them, our implementation allows adding, removing, or changing their order without modifying
422 the code. Structuring code into graph functions enable easy reuse of code, customisation,
423 and introduction of new processing steps. Graph functions are wrapped in a class for
424 validation, enabling SWMManywhere to identify if a set of graph functions to be applied is
425 valid *a priori*. Graph functions are stored in a registry object to enable easy access. We
426 provide a description of all graph functions in the documentation online (SWMManywhere
427 documentation, 2024). However, users may also customise the selection and order of graph
428 functions, or create new ones, as described in the online documentation, to fit their
429 requirements.

430 Processes or operations described in Sections 2.1.1 and 2.1.2 that are used by but not
431 implemented natively within the tool are described in Table 3.

432 *Table 3: List of tools for specific tasks in our SWMManywhere implementation.*

TASK	SOFTWARE	REFERENCE
DEM CONDITIONING	Whitebox	(Lindsay, 2016b)
FLOW DIRECTION CALCULATIONS	Whitebox	(Lindsay, 2016b)
SUB-CATCHMENT DELINEATION FROM FLOW DIRECTIONS	PyFlwDir	(Eilander, 2022)
SUB-CATCHMENT SLOPE CALCULATION	PyFlwDir	(Eilander, 2022)
OSM DATA RETRIEVAL	OSMnx	(Boeing, 2017)
GRAPH OPERATIONS	Networkx	(Hagberg et al., 2008)

433

434 To accommodate ease of use for a wide range of users with different levels of programming
 435 experience, we provide a command-line interface (CLI) for the software. More experienced
 436 users can take advantage of the modularity of SWMManywhere for more advanced
 437 customisation of the workflow. The CLI works with a configuration file that enables a user to
 438 change parameter values and functionality. The minimal essential requirements that this file
 439 must contain are a project name, a base directory, and a bounding box. The configuration
 440 file provides a centralised location to perform customisations including changing the
 441 selection/ordering of graph functions, changing parameter values (see Table 1), file locations
 442 of a real network to compare against (see Section 2.1.3) and which metrics to calculate (see
 443 Table 2), a starting graph if not using downloaded street data, and any running settings for
 444 the SWMM simulation. A variety of online tutorials explain the procedure to make such
 445 customisations.

446 SWMManywhere provides a capability to write simple SWMM model files (typically with a
 447 .inp file extension) that have been synthesised via the various graph functions used. It also
 448 provides a wrapper of the PySWMM software (McDonnell et al., 2020), which enables calling
 449 the SWMM software and interacting with its simulations from Python. Thus, in addition to the

450 UDM synthesis, writing, running, and calculating metrics if real network information exists
451 are carried out during the command line call.

452 Precipitation data is frequently identified as a critical factor in UDM simulations (Ochoa-
453 Rodriguez et al., 2015), however, there are currently no open global datasets that provide
454 the high frequency monitoring needed to drive these models and so precipitation must be
455 user-provided if deviating from the default storm provided as part of the tool.

456 2.2 Sensitivity analysis

457 Sensitivity analysis is used to examine how output variations can be attributed to input
458 variations, typically expressed as sensitivity indices for each model parameter (Pianosi et al.,
459 2016). While popular reviews in the environmental sciences define sensitivity analysis as
460 specific to model input/outputs (Saltelli et al., 2008, 2019; Pianosi et al., 2016), it can equally
461 be applied to any generic parameterised workflow, such as SWMMAnywhere. As defined in
462 Table 1, there are a wide variety of parameters that must be selected, many of which do not
463 have values that could be easily measured or derived, and thus are useful candidates for
464 sensitivity analysis.

465 In general, it is recognised that, to robustly conduct sensitivity analysis, a global method
466 should be used, and the variability of the calculated indices should be checked to ensure
467 that the number of samples is sufficient (Saltelli et al., 2019). Because of the presumed high
468 level of dependency in the SWMMAnywhere workflow (for example, hydraulic design
469 depends entirely on network topology, which in turn depends on outfall and manhole
470 identification), we also calculate second order indices to better capture interactions between
471 parameters (Herman and Usher, 2017). To implement sensitivity analysis for
472 SWMMAnywhere, we use the SALib software (Herman and Usher, 2017), which provides a
473 variety of global methods for sampling parameter ranges and calculating sensitivity indices
474 natively in Python. In this study we use the Sobol method (Sobol, 1993) due to its
475 widespread use and recognised robustness of results providing that a sufficient number of
476 samples can be investigated (Pianosi et al., 2016). 18 parameters are sampled, indicated in

477 Table 1, and 16 metrics, Table 2, are evaluated. Thus, the overall approach is to perform
478 parameter sampling, run SWMManywhere with the parameters of each sample, calculate the
479 performance metrics between the synthesised and real UDMs, and calculate sensitivity
480 indices.

481 Sobol sensitivity analysis that includes second order interactions with SALib requires taking
482 samples equal to,

$$N = n * (2m + 2) \quad (2),$$

483 where N is the total number of samples (or SWMManywhere calls), m is the number of
484 parameters, and n is the number of Sobol sequence samples to generate (preferably a
485 power of 2). In this experiment we set n to 2^{10} (1024), m is 18, resulting in N of 38912. As
486 demonstrated in Pianosi et al., (2016), this many evaluations ($m * 1000$) are towards the
487 upper limit of what is found in the literature. We take this opportunity to note a further benefit
488 of sensitivity analysis in the context of SWMManywhere as a global tool, which is that testing
489 it under such a large and diverse range of parameters further guarantees robustness of the
490 software implementation in locations not tested.

491 **3 Case studies**

492 In this study, we evaluate our proposed workflow by comparing the SWMM simulation
493 results obtain from using the synthetic UDM with those of the real UDM for the Cran Brook,
494 London, UK (Babovic and Mijic, 2019). We then perform sensitivity analysis in other
495 locations to examine the transferability of results and parameters. We use seven UDMs
496 around the town of Bellinge, Denmark, as delineated by Farina et al., (2023). These data
497 were selected because they are openly available and demonstrate results over a wide range
498 of scales (Pedersen et al., 2021). The properties of the case study networks are presented in
499 Table 4.

500 *Table 4: Summary of networks tested and their properties*

Network	Number of nodes	Number of edges	Impervious percentage
Cran Brook	6931	6965	27
Bellinge 1	142	150	36
Bellinge 2	118	117	33
Bellinge 3	52	51	25
Bellinge 4	46	45	32
Bellinge 5	45	46	40
Bellinge 6	36	35	32
Bellinge 7	15	14	34

501

502 A key feature of many UDM is the presence of hydraulic structures such as weirs, orifices,
 503 storages, or pumps. There is extensive evidence from the sewer network simplification
 504 literature that capturing and parameterising these structures is critical towards reproducing
 505 the behaviour of the real network (Thrysoe et al., 2019; Dobson et al., 2022). However,
 506 SWMManywhere currently does not attempt to estimate the locations or hydraulic properties
 507 of any such structures. We acknowledge that this could be a significant limitation and hope
 508 to add this behaviour in future work. In this paper, we replace the hydraulic structures and
 509 storage nodes in the real models with simple and uniform nodes to better assess the
 510 SWMManywhere workflow as designed. Furthermore, the hydraulic properties of sub-
 511 catchments (specifically, the Manning’s roughness coefficient and depression storage of
 512 both impervious and pervious areas) are a significant source of uncertainty and typically
 513 calibrated or set arbitrarily (Deletic et al., 2012), thus we set these at the same values for all
 514 networks to ensure comparability.

515 The precipitation event we use to demonstrate SWMManywhere is the largest storm in the
 516 openly available Bellinge data (Pedersen et al., 2021).

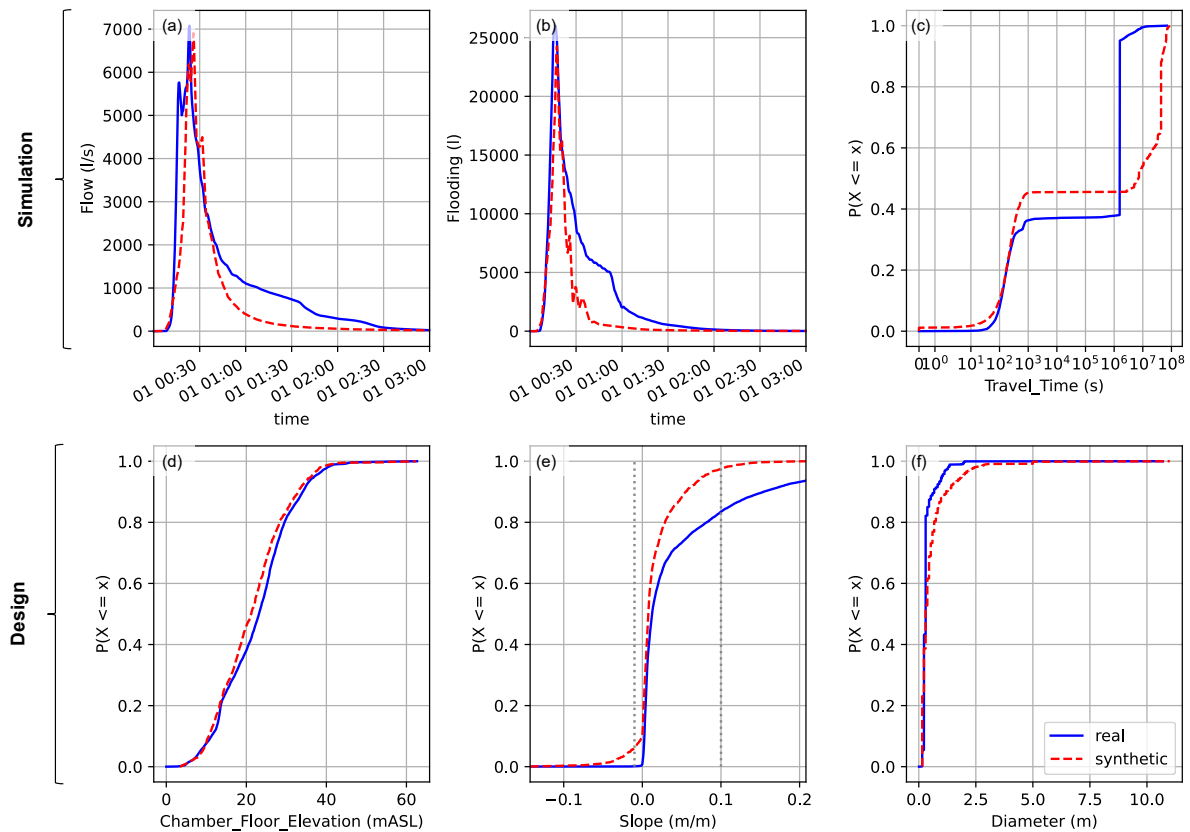
517 Workflow evaluations were performed on the Imperial College High Performance Computing
518 facilities (see Acknowledgements). Hardware used was typically AMD EPYC 7742 (128
519 cores, 1TB RAM per node), although this varied based on availability. On one of these
520 machines, for a single workflow evaluation in the Cran Brook case study, downloading and
521 data preprocessing takes ten seconds (except for buildings, which are national datasets and
522 so download speeds will vary significantly depending on the country), evaluating graph
523 functions and writing the UDM to SWMM format takes around two minutes (deriving sub-
524 catchments and deriving network topology are the slowest individual steps at 20 seconds
525 each), simulation in SWMM takes eight minutes, and evaluating metrics takes two minutes
526 (dominated by the *K-S test for node betweenness, mKN* which took over one minute). Run
527 times for all Bellinge case studies were dramatically quicker owing to the far smaller UDM
528 sizes.

529 The code used to perform this experiment and results required to reproduce the figure
530 results in Section 4 are openly shared in a separate repository (Dobson et al., 2024b).

531 **4 Results**

532 4.1 Proof-of-concept examination

533 We focus this section on a synthesised model selected from our sensitivity analysis sampling
534 (Section 4.2) that performed well across a range of metrics to assess SWMManywhere's
535 ability to generate a high-quality UDM and raise methodological points of interest. Figure 4
536 plots a flow and flooding timeseries and diameter, elevation, slope, and travel time
537 distributions for the Cran Brook network to provide a detailed comparison of the real and
538 synthetic UDM.



539

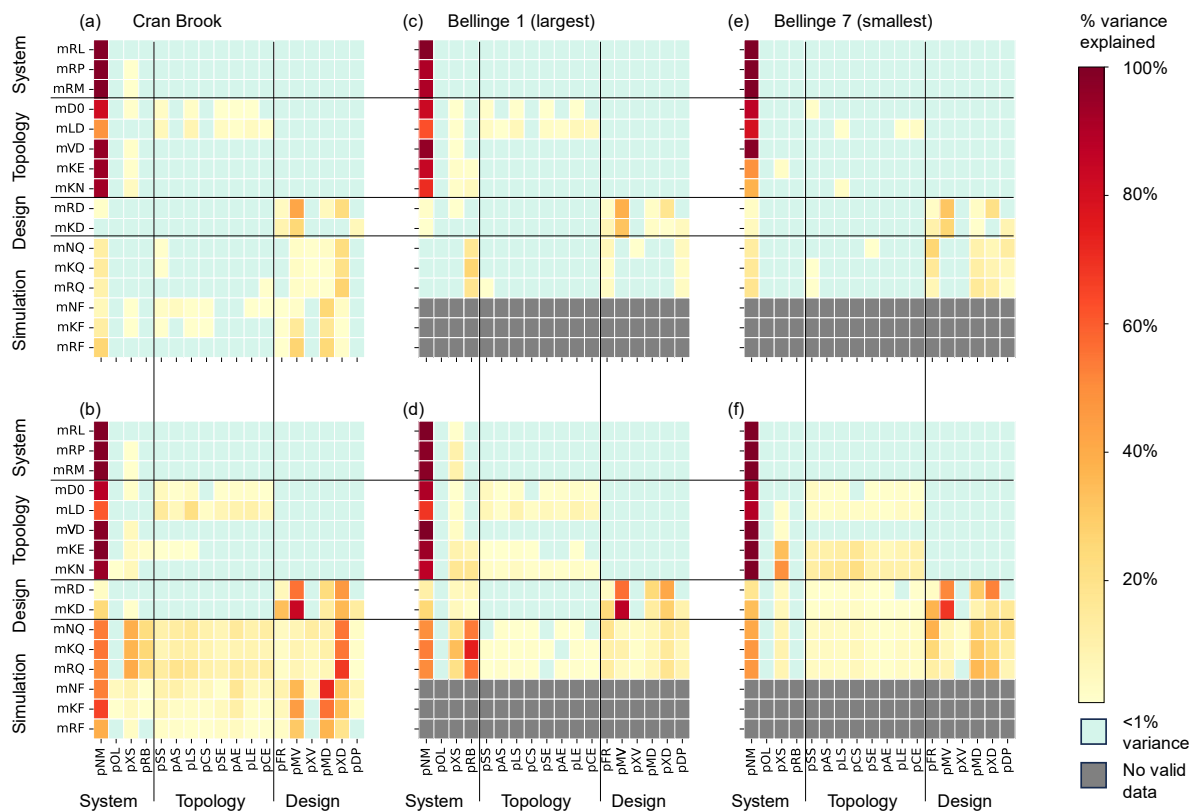
540 *Figure 4: Demonstration plot of a high performance synthetic UDM. Red dashed lines represent synthetic data,*
 541 *while solid blue represents the real UDM simulations. Grey lines on the slope plot (e) show the target design*
 542 *range.*

543 Figure 4a shows flow at the network outfall, while Figure 4b shows the total flooded volume
 544 across the network. We see that the maximum values of both are captured with accuracy,
 545 however, the falling limb for both recedes more quickly in the synthetic network than in the
 546 real UDM simulations. The synthetic network has consistently larger diameters (Figure 4f)
 547 than the real, while chamber floor elevations (Figure 4d) are well matched. Synthetic pipe
 548 slopes (Figure 4e) are lower, although we observe that these are primarily within the grey
 549 dashed lines which show the target design range (Chahinian et al., 2019). The average
 550 travel time from each node to the outfall (Figure 4c) shows distinctively different patterns
 551 across the distribution, with a good match for the quickest third of nodes, the synthetic UDM
 552 quicker for the middle third (because of the larger diameters), and the real UDM quicker for
 553 the slowest third. Although not shown, the total runoff from manhole sub-catchments in both

554 the real and synthetic models is within 2% of each other, which is true for all synthesised
 555 UDMs.

556 4.2 Sensitivity analysis, Cran Brook

557 SWMMAnywhere parameters, see Table 1, were sampled using a Sobol sampling scheme,
 558 see Section 2.2, to enable a global sensitivity analysis using the Sobol method. The findings
 559 of this analysis for Cran Brook, the sensitivity indices, are presented in Figure 5a-b. Two
 560 other locations (Figure 5 c-f) are discussed in Section 4.2, with other locations in full
 561 presented in Supplemental Figure S1.



562
 563 *Figure 5: Heatmap demonstrating the sensitivity indices (a) of first order variance (S1) of a metric (y-axis)*
 564 *attributable to a parameter (x-axis) based on simulations in the Cran Brook network, (b) of total variance (ST)*
 565 *attributable to a parameter based on simulations in the Cran Brook network. Red indicates more sensitive and*
 566 *yellow less sensitive. Blue indicates less than 1% variance explained. (c, d, e, f), shows equivalent of (a) and (b)*
 567 *respectively, but for the Bellinge 1 and Bellinge 7 networks. Grey indicates no sensitivity indices could be*
 568 *calculated because no flooding occurred.*

569 In Figure 5 we show the first order variance (S1) of each metric (as listed in Table 2)
 570 attributable to each parameter (Figure 5a), and the total variance (ST) attributable (Figure
 571 5b). We see that sensitivity is widespread, with every parameter exhibiting at a total variance
 572 attributable of >1% for at least one metric. We also see that sensitivity is overwhelmingly

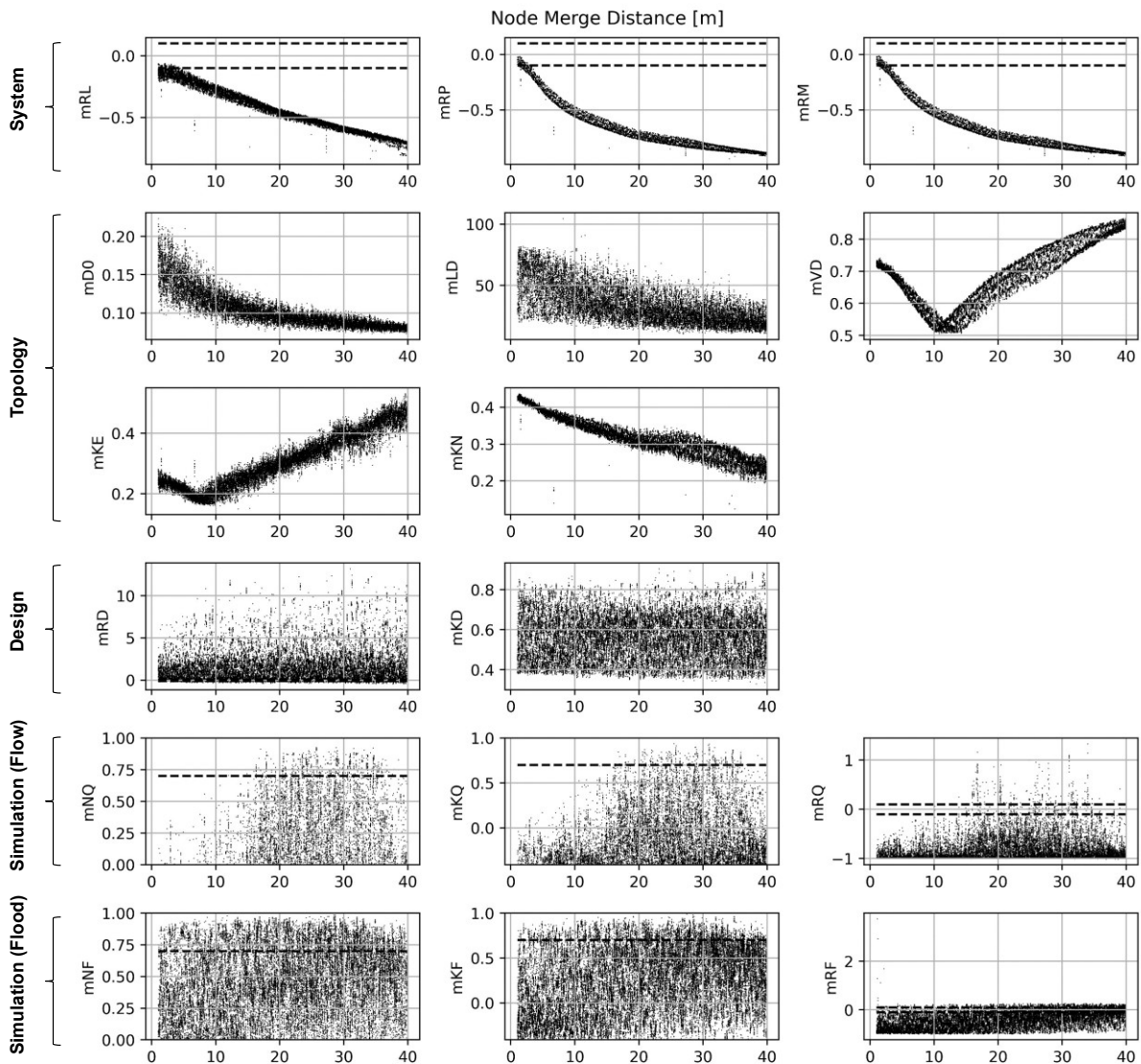
573 occurring through interactions (i.e., sensitivities present in Figure 5b but not in Figure 5a),
574 with some notable exceptions: *node merge distance* (*pNM*), *minimum velocity* (*pMV*),
575 *minimum* (*pMD*) and *maximum chamber depth* (*pXD*). First order sensitivity indicates that
576 the parameter is sensitive regardless of other parameter values, *pMV* and *pNM* are evidently
577 dominant in their influence on pipe design while *pNM* is discussed below. Second order
578 variance indices were also calculated, but not included because their confidence intervals
579 were prohibitively large.

580 Across metrics the *node merge distance* is the most sensitive parameter, impacting both
581 system description metrics (top rows), topology metrics (middle rows), and simulation
582 metrics (bottom rows). It is a sensitive parameter because it interacts with three key
583 elements in SWMManywhere:

- 584 - It influences manhole placement, which is also impacted by *max street length* (*pXS*,
585 another sensitive parameter).
- 586 - It impacts which nodes can drain to where, which is also impacted by *river buffer*
587 *distance* (*pRB*, another sensitive parameter).
- 588 - It can significantly alter how the road layout is translated into potential pipes, which
589 no other parameter does. For example, two adjacent roads running parallel may not
590 have a driving connection between them, and thus no potential pipe may span them,
591 but if these nodes are merged then a pipe could span them.

592 In addition to the dominance of these three parameters (*node merge distance*, *max street*
593 *length* and *river buffer distance*), we see many other intuitively appropriate sensitivities.
594 System metrics are sensitive to system parameters, topological metrics to topological
595 parameters, and design metrics to design parameters. We also find that flow simulation
596 metrics are sensitive to parameters relating to network topology, indicating that topology is
597 primarily influencing the global behaviour of the UDM. In contrast, we see that flood
598 simulation metrics are more sensitive to design parameters, indicating that design is
599 primarily influencing the local behaviour of the UDM.

600 We provide a specific examination of *node merge distance*, selected because it is the most
 601 sensitive parameter, to illustrate how SWMMAnywhere can be used to provide a detailed
 602 parametric exploration. We plot the parameter value of *node merge distance* against each
 603 metric value for all sampled points in Figure 6. We see clear evidence of first order sensitivity
 604 in line with those reported in Figure 5a-b.



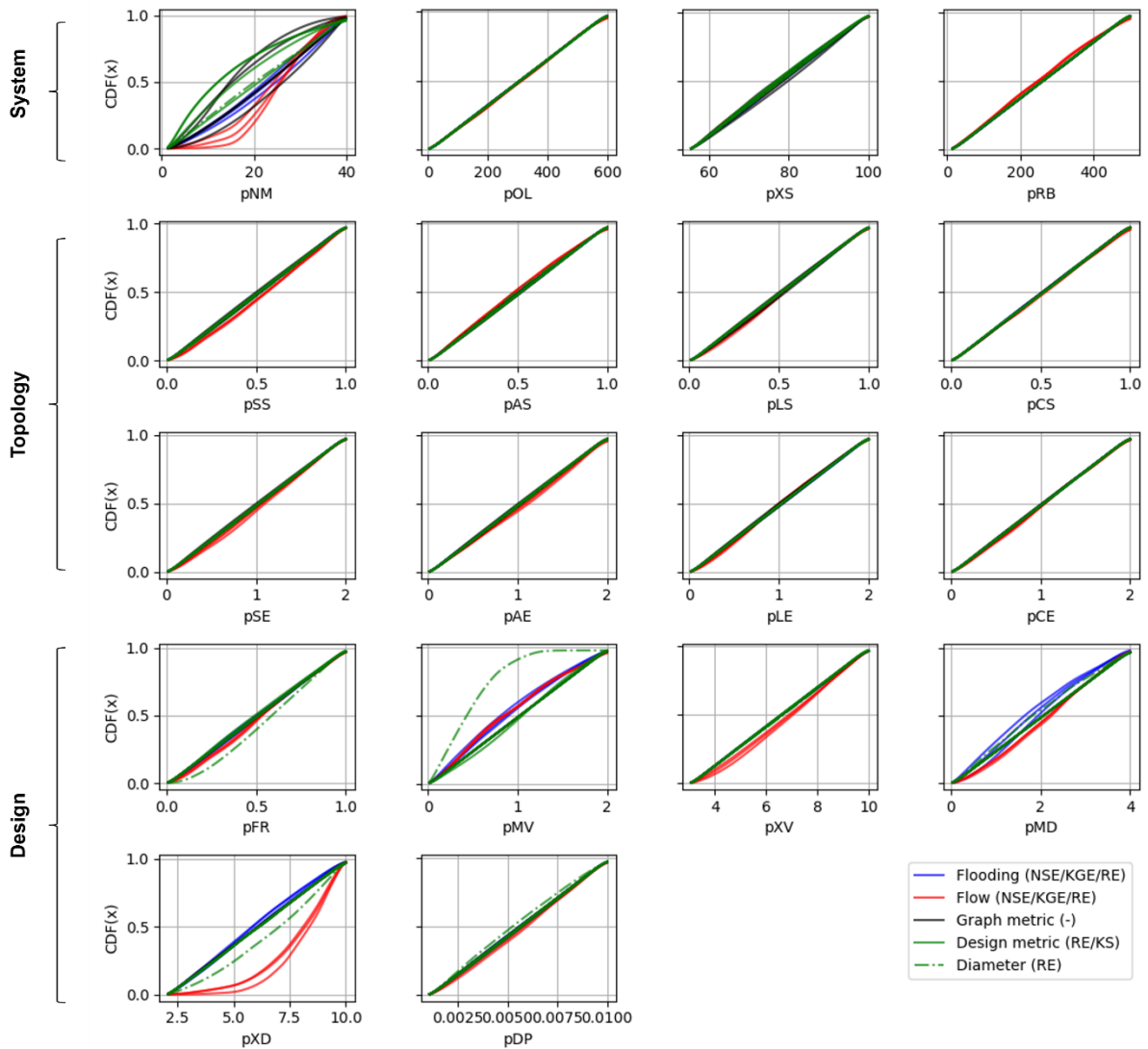
605

606 *Figure 6: Node merge distance parameter value plotted against all evaluated performance metrics. Based on*
 607 *simulations in the Cran Brook network. Panels showing NSE or KGE are clipped at 0.0 and -0.41 respectively,*
 608 *which indicates the performance of taking the mean value of observations as the simulation. Dashed lines for*
 609 *KGE, NSE, relative error indicate a region of 'behavioural' performance, that is, values >0.7 (KGE, NSE) or within*
 610 *+/- 0.1 (relative error).*

611 Figure 6 indicates some evidence of identifiable parameter values, e.g., we observe that the
 612 *node merge distance* should fall around 25m for the simulation flow metrics. However, this

613 value can vary depending on which metric is used, for example, System metrics (*mRL*, *mRP*,
614 and *mRM*) and some topology metrics (*mVD*, *mKE*, *mKN*) indicate better performance when
615 *node merge distance* is around 0-15m.

616 It can be more informative to investigate whether parameters are identifiable using a
617 Gaussian kernel density estimate (KDE), which can be used to create a cumulative density
618 function for each parameter and can be weighted by different metrics. For example, in Figure
619 7, top left panel (*pNM*), weighting the KDE by flow simulations (red lines), we can see that
620 75% of the distribution indicates that *node merge distance* should be greater than 20m,
621 agreeing with Figure 6. The KDE plots further highlight identifiability for a range of other
622 parameters, however, as with *node merge distance*, in most cases there can be
623 disagreement depending on which metric is used for weighting.



624

625 *Figure 7: Gaussian KDE cumulative density functions for parameters, weighted by different metrics evaluated on*
 626 *the Cran Brook network. Metrics are grouped by colour to highlight different behaviours.*

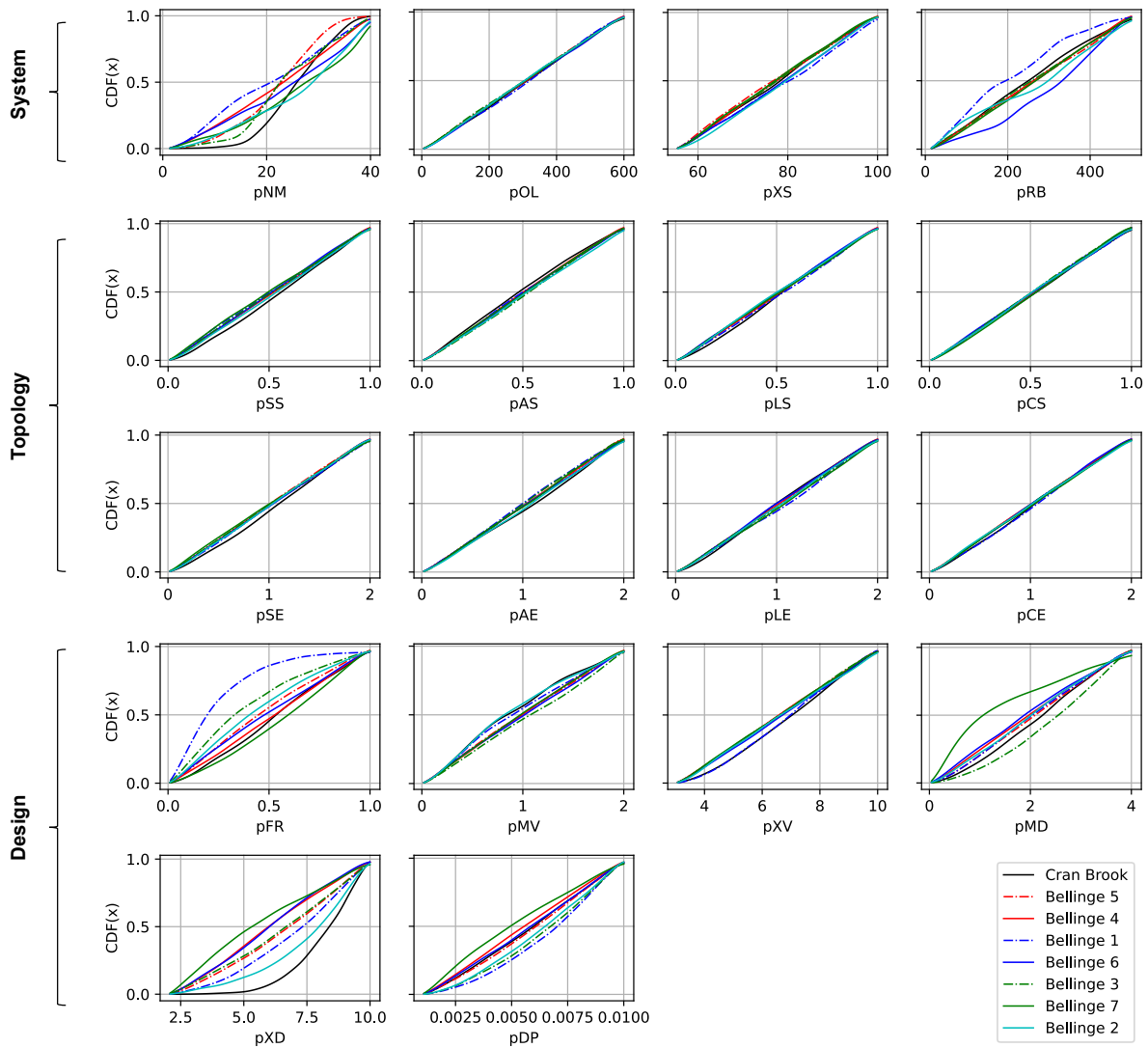
627 **4.3 Sensitivity analysis, other locations**

628 In Figure 5 c-f we show the sensitivity analysis results for the Bellinge 1 and 7 networks,
 629 which are the largest and smallest networks in the Bellinge dataset, respectively. Results for
 630 the other Bellinge UDMs are shown in Supplemental Figure S1, although do not
 631 meaningfully differ from the observations below.

632 In general, we see many similarities between the two analyses, including high sensitivity of
 633 *node merge distance*, more sensitivity occurring through interactions (Figure 5 c and e) than
 634 in first order (Figure 5 d and f). In contrast, we see less significance of network topology
 635 parameters across all metrics, which we can likely be attributed to smaller sizes of both

636 Bellinge networks are comparing to the Cran Brook network resulting in availability of fewer
637 topological configurations, thus less significance in terms of impacting metrics. We note that
638 no indices for flooding metrics could be calculated because the network did not experience
639 flooding under the precipitation timeseries used.

640 In Figure 8 we show the KDE estimates of parameter distributions for each network,
641 weighted by the NSE flow metric (mNQ). In contrast to Figure 7, we see stronger agreement
642 across networks than across metrics for weighting. For example, *max fr* (pXF), *precipitation*
643 (pDP), *max depth* (pXD), tend towards aligned parameter distributions across most
644 networks. Despite this, we also see some sensitive parameters with less agreement across
645 networks. For example, *min v* (pMV), *max street length* (pXS), and *node merge distance*
646 (pNM) have unaligned but identifiable parameter values. We also see that many parameters
647 do not have clearly defined distributions for most networks but do for one/few. For example,
648 *river buffer distance* appears to have a clearly defined distribution for Cran Brook and
649 Bellinge 2, while no other networks do. We do not see clear parameter distributions for
650 network topology parameters, despite their sensitivity demonstrated in Figure 5.



651

652 *Figure 8: Gaussian KDE cumulative density function for parameters for each location. Weighted by outfall flow*
 653 *NSE.*

654 **5 Discussion**

655 **5.1 Development of SWMManywhere**

656 In this study, we provide new insight into the intricacies of UDM synthesis through
 657 application of our proposed SWMManywhere workflow and performing extensive sensitivity
 658 analysis.

659 We demonstrate in Figure 4 that reasonable simulations are achievable, with NSE values of
 660 >0.7 for both outfall flow and flooding, Figure 6. The implementation based on Duque et. al.,
 661 (2022)'s pipe-by-pipe method results in high efficiency UDMs, although we observe that the

662 synthesised UDMs are perhaps too efficient as they drain the network too quickly, see flow
663 and flood simulations in Figure 4. This finding suggests that inefficiencies seen in the real
664 network reflect the additional constraints not captured by data sources that we employ in our
665 workflow, for example, incremental construction of the network (Rauch et al., 2017). Despite
666 such shortcomings, we recommend that sensitivity analysis is a necessary precursor to
667 introducing any further complexity.

668 The sensitivity analysis results, Figure 5, show widespread and intuitively sensible sensitivity
669 of all parameters, including those introduced as technical innovations of this paper: enabling
670 slope inclusion within the MSA and contributing area as a factor in the network topology
671 derivation (p_{SS} , p_{CS} , p_{SE} , p_{CE}). We also highlight the dominant sensitivity of *node merge*
672 *distance* (p_{NM}), which influences manhole locations, outfall locations, and underlying street
673 graph preprocessing. Manhole locations are well established to be important factors
674 (Chahinian et al., 2019; Blumensaat et al., 2012), while to our knowledge this is the first
675 UDM synthesis study that treats outfall locations as an explicit unknown. The importance of
676 the underlying street graph that *node merge distance* controls is intuitively sensible, as a
677 UDM synthesis can only ever be as good as the potential pipe-carrying locations that it
678 begins with. These findings indicate a promising outlook for UDM synthesis, as manhole
679 locations, outfall locations, and the street graph are all surface elements whose estimation
680 will only improve with improved satellite imagery and machine learning. Furthermore, in
681 cases where SWMManywhere is to be applied to a local area, surveying these surface
682 elements is likely to be far less costly than a below-ground network survey.

683 5.2 Transferability of SWMManywhere

684 A key motivation for performing sensitivity analysis is in identifying behavioural parameter
685 ranges. In an ideal case, behavioural parameter ranges align across metrics and locations,
686 thus implying that parameter choices are good under any condition. Figure 7 and Figure 8
687 demonstrate that we do not see clear evidence of this for either metrics or locations
688 respectively. Figure 5 demonstrates that parameters are generally sensitive through

689 interactions, rather than through first order effects, which limits the ability to provide clear
690 advice on behavioural ranges. Although second order effects were calculated, the
691 confidence intervals were such that no conclusions could be drawn, and we estimate that
692 multiple magnitudes more samples would be required to provide definitive results, which is
693 outside the scope of this paper, but future work may investigate. Parameters that have high
694 first order sensitivity provide some clear advice, for example, *node merge distance* values
695 should be between 20m-35m to provide good flow simulation metrics in a variety of
696 locations. However, the dominant finding on parameter transferability is that the panacea of
697 arriving to a single 'correct' UDM through a synthesis approach is false. Indeed, we believe
698 that widespread findings of equifinality in hydraulic calibration of real UDMs, (Huang et al.,
699 2022; Sytsma et al., 2022) supports that the idea of having a single 'correct' UDM that is
700 based on survey information (rather than synthesis) is also false. We propose that data
701 uncertainty will remain a fundamental element of UDM, synthetic or otherwise, for the
702 foreseeable future.

703 We therefore advocate for an approach to UDM that is uncertainty driven. Rather than
704 narrowly focussing on aligning synthetic with real UDMs, a synthetic UDM may most
705 appropriately be considered one hypothesis for the underlying system. Further
706 developments to SWMMAnywhere should thus seek to synthesise UDMs that are plausible
707 hypotheses, possibly through a more iterative approach that refines the UDM based on
708 simulation data only, for example, by assessing SWMM continuity errors. In a no field data
709 setting, the focus could shift to, for example, various climate scenarios or future urban
710 development, to study an ensemble of plausible UDMs and explore their likely outcomes. If
711 such studies would prohibitively increase simulation time, a range of network complexity
712 reduction techniques have been demonstrated for UDMs (Farina et al., 2023; Palmitessa et
713 al., 2022), including as part of an uncertainty ensemble approach (Dobson et al., 2022;
714 Thrysøe et al., 2019).

715 To ensure that our proposed workflow is applicable at the global scale, we have deliberately
716 avoided some data, for example design regulations or a higher resolution DEM, that are
717 commonly available at national scales. In local applications, however, we do recommend
718 exploring utilising the best quality data available and adapting the underlying datasets or
719 parameter assumptions, which our SWMManywhere implementation supports. Nevertheless,
720 we caution that this may not provide the certainty that one might expect. For example, as our
721 KDE parameter estimates demonstrate in Bellinge, Denmark (Figure 8), design regulations,
722 which are parameters that are country and region specific, do not show agreement across
723 UDMs in the same locale.

724 5.3 Outlook and limitations

725 The modular graph function-based architecture of SWMManywhere makes it easy to extend
726 or customise, thus we hope that it may become a centralised location for the synthetic UDM
727 community. We see a variety of potential improvements that may be introduced to increase
728 the realism of synthesised UDMs, although we stress the importance of performing
729 sensitivity analysis before investing time in creating complicated customisations. In addition
730 to better identification of surface elements described above, other surface factors such as
731 hydraulic structures are well established to play a dominant role in UDM behaviour (Thryssøe
732 et al., 2019; Dobson et al., 2022). SWMManywhere does not attempt to synthesise these
733 structures, and they are omitted from the analysis performed in this paper. However,
734 structures such as weirs may be identifiable from satellite imagery, while including pumps
735 may form an additional element in the network topology derivation, as has been
736 demonstrated for sanitary sewer networks (Khurelbaatar et al., 2021).

737 An immediate extension to the behaviour of SWMManywhere that we are exploring is
738 around water quality. Recent literature demonstrates the feasibility of quantifying urban
739 pollution deposition on roads (Revitt et al., 2022), which could be included as an optional
740 extension, thus providing the much-needed transport element to link deposition with in-river
741 pollution. We anticipate that a key difficulty of such an approach would be in identifying

742 validation data, since sampling water quality at urban drainage outfalls during a storm is
743 dangerous to do in person. For example, while the English Environment Agency's
744 harmonised water quality sampling database contains over 60 million pollution sample
745 records since 2000 (Open water quality archive datasets (WIMS), 2024), just 0.4% are of
746 urban drainage outfalls, and only 25% of these have occurred since 2010, reflecting the
747 diminishing focus on non-compliance monitoring observed across England (Dobson et al.,
748 2021). Further improvements towards capturing water quality may also focus on
749 representing combined or misconnected systems, linking with the synthetic sanitary sewer
750 network literature (Duque et al., 2022).

751 A clear limitation of the case studies demonstrated in this paper is that they are based in
752 temperate and wealthy European countries, this is particularly problematic when considering
753 that street graph and building footprint data uncertainty will be more significant in nearly any
754 other type of region. We reached out to a variety of urban drainage modellers in both
755 industry and research but were not able to extend our case study selection further and
756 instead identified a significant paucity of publicly available reliable SWMM models. While the
757 SWMM website hosts a variety of useful example models, these aim to build understanding
758 about representing different elements of drainage networks, rather than providing a suite of
759 real test cases. Ultimately, SWMManywhere and other synthetic UDM tools will not be
760 trusted at global scales until they have been demonstrated on a wide variety of case studies.
761 Thus, we call for collaborators who can either share their SWMM models openly or are
762 willing to demonstrate SWMManywhere for their models to reach out that we may create a
763 more robust demonstration of UDM synthesis and verify that understandings created are
764 sustainable.

765 **6 Conclusion**

766 In this paper we present a workflow, SWMManywhere, that can synthesise an urban
767 drainage network model (UDM) and simulate it in SWMM, anywhere globally. We test the

768 parameters of SWMMAnywhere using sensitivity analysis to understand the dominant
769 processes involved in synthesising UDMs. Our results revealed three key findings:

- 770 1. The SWMMAnywhere workflow can synthesize high quality UDM at a range of spatial
771 scales. The parameters that can be used to tune SWMMAnywhere behave in
772 intuitively sensible ways, verifying its implementation.
- 773 2. We find that parameters controlling surface elements such as manhole locations,
774 street layout, and network outfalls are the most sensitive, and thus should be the key
775 focus of uncertainty reduction. Encouragingly, the identification of these elements is
776 also the most likely to improve in the foreseeable future.
- 777 3. UDM synthesis is sensitive to all parameters and these parameters primarily
778 influence outputs through second order or higher interactions, revealing UDM
779 synthesis to be a more complex process than previously recognised. Additionally, we
780 recommend that an ensemble approach would be appropriate for practical
781 applications to more appropriately reflect the inherent uncertainty of the underlying
782 system.

783 We hope that the urban drainage community will use SWMMAnywhere to further explore the
784 complexity of UDM synthesis, develop robust interventions in areas without existing UDM
785 data, and do so in a more open and reproducible scientific environment.

786 **7 Acknowledgements**

787 BD, TJ, DA, TC were involved in theoretical formulation of the SWMMAnywhere
788 methodology. BD, DA, TC were involved in software development, with further support
789 provided by Imperial College's Research Software Engineering service. BD, TJ, TC were
790 involved in the experimental formulation and sensitivity analysis. BD, TJ, TC, DA were
791 involved in drafting and editing the manuscript. We are also grateful to Ana Mijic for their
792 insightful comments on the manuscript that have improved the paper.

793 BD is funded through the Imperial College Research Fellowship scheme, which also funded
794 the software development. TJ time was supported by the UK Natural Environment Research
795 Council-funded CAMELLIA project (grant no. NE/S003495/1). TJ publishes with the
796 permission of the Executive Director of the British Geological Survey. We acknowledge
797 computational resources and support provided by the Imperial College Research Computing
798 Service (<http://doi.org/10.14469/hpc/2232>).

799 **8 Data availability statement**

800 The software implementation of SWMManywhere is an open-source repository available at
801 <https://github.com/ImperialCollegeLondon/SWMManywhere> (last accessed 2024-10-11). The
802 documentation for SWMManywhere can be found at
803 <https://imperialcollegelondon.github.io/SWMManywhere/> (last accessed 2024-10-11). The
804 results of the paper's experiments and code to perform sensitivity analysis and plots is
805 available at https://github.com/barneydobson/swmmanywhere_paper (last accessed 2024-
806 10-11).

807 **9 References**

- 808 Arrighi, C. and Campo, L.: Effects of digital terrain model uncertainties on high-resolution
809 urban flood damage assessment, *J. Flood Risk Manag.*, 12,
810 <https://doi.org/10.1111/jfr3.12530>, 2019.
- 811 Babovic, F. and Mijic, A.: The development of adaptation pathways for the long-term
812 planning of urban drainage systems, *J. Flood Risk Manag.*, 12,
813 <https://doi.org/10.1111/jfr3.12538>, 2019.
- 814 Bach, P. M., Rauch, W., Mikkelsen, P. S., McCarthy, D. T., and Deletic, A.: A critical review
815 of integrated urban water modelling - Urban drainage and beyond, *Environ. Model. Softw.*,
816 54, 88–107, <https://doi.org/10.1016/j.envsoft.2013.12.018>, 2014.
- 817 Bach, P. M., Kuller, M., McCarthy, D. T., and Deletic, A.: A spatial planning-support system
818 for generating decentralised urban stormwater management schemes, *Sci. Total Environ.*,
819 726, 138282, <https://doi.org/10.1016/j.scitotenv.2020.138282>, 2020.
- 820 Bertsch, R., Glenis, V., and Kilsby, C.: Urban flood simulation using synthetic storm drain
821 networks, *Water (Switzerland)*, 9, <https://doi.org/10.3390/w9120925>, 2017.
- 822 Blumensaat, F., Wolfram, M., and Krebs, P.: Sewer model development under minimum
823 data requirements, *Environ. Earth Sci.*, 65, 1427–1437, <https://doi.org/10.1007/s12665-011-1146-1>, 2012.
- 825 Boeing, G.: OSMnx: New methods for acquiring, constructing, analyzing, and visualizing
826 complex street networks, *Comput. Environ. Urban Syst.*, 65, 126–139,

- 827 <https://doi.org/10.1016/j.compenvurbsys.2017.05.004>, 2017.
- 828 Butler, D. and Davies, J. w.: *Urban Drainage* 2nd Edition, 566 pp., 2004.
- 829 Chahinian, N., Delenne, C., Commandré, B., Derras, M., Deruelle, L., and Bailly, J. S.:
830 Automatic mapping of urban wastewater networks based on manhole cover locations,
831 *Comput. Environ. Urban Syst.*, 78, 101370,
832 <https://doi.org/10.1016/j.compenvurbsys.2019.101370>, 2019.
- 833 Chegini, T. and Li, H. Y.: An algorithm for deriving the topology of belowground urban
834 stormwater networks, *Hydrol. Earth Syst. Sci.*, 26, 4279–4300, [https://doi.org/10.5194/hess-](https://doi.org/10.5194/hess-26-4279-2022)
835 [26-4279-2022](https://doi.org/10.5194/hess-26-4279-2022), 2022.
- 836 Coxon, G., McMillan, H., Bloomfield, J. P., Bolotin, L., Dean, J. F., Kelleher, C., Slater, L.,
837 and Zheng, Y.: Wastewater discharges and urban land cover dominate urban hydrology
838 signals across England and Wales, *Environ. Res. Lett.*, 19, 084016,
839 <https://doi.org/10.1088/1748-9326/ad5bf2>, 2024.
- 840 Crippen, R., Buckley, S., Agram, P., Belz, E., Gurrola, E., Hensley, S., Kobrick, M., Lavallo,
841 M., Martin, J., Neumann, M., Nguyen, Q., Rosen, P., Shimada, J., Simard, M., and Tung, W.:
842 NASADEM GLOBAL ELEVATION MODEL: METHODS AND PROGRESS, *Int. Arch.*
843 *Photogramm. Remote Sens. Spat. Inf. Sci.*, XLI-B4, 125–128, [https://doi.org/10.5194/isprs-](https://doi.org/10.5194/isprs-archives-XLI-B4-125-2016)
844 [archives-XLI-B4-125-2016](https://doi.org/10.5194/isprs-archives-XLI-B4-125-2016), 2016.
- 845 Deletic, A., Dotto, C. B. S., McCarthy, D. T., Kleidorfer, M., Freni, G., Mannina, G., Uhl, M.,
846 Henrichs, M., Fletcher, T. D., Rauch, W., Bertrand-Krajewski, J. L., and Tait, S.: Assessing
847 uncertainties in urban drainage models, *Phys. Chem. Earth*, 42–44, 3–10,
848 <https://doi.org/10.1016/j.pce.2011.04.007>, 2012.
- 849 Dobson, B., Jovanovic, T., Chen, Y., Paschalis, A., Butler, A., and Mijic, A.: Integrated
850 modelling to support analysis of COVID-19 impacts on London’s water system and in-river
851 water quality, *Front. Water*, 3, 26, <https://doi.org/10.3389/frwa.2021.641462>, 2021.
- 852 Dobson, B., Watson-Hill, H., Muhandes, S., Borup, M., and Mijic, A.: A Reduced Complexity
853 Model With Graph Partitioning for Rapid Hydraulic Assessment of Sewer Networks, *Water*
854 *Resour. Res.*, 58, <https://doi.org/10.1029/2021WR030778>, 2022.
- 855 Dobson, B., Alonso-Álvarez, D., and Chegini, T.: SWMManywhere,
856 <https://doi.org/10.5281/zenodo.13837741>, September 2024a.
- 857 SWMMAnywhere documentation: <https://imperialcollegelondon.github.io/SWMMAnywhere/>,
858 last access: 4 October 2024.
- 859 Dobson, B., Alonso-Álvarez, D., and Chegini, T.: SWMMAnywhere sensitivity analysis,
860 <https://doi.org/10.5281/zenodo.13918627>, September 2024b.
- 861 Duque, N., Bach, P. M., Scholten, L., Fappiano, F., and Maurer, M.: A Simplified Sanitary
862 Sewer System Generator for Exploratory Modelling at City-Scale, *Water Res.*, 209, 117903,
863 <https://doi.org/10.1016/j.watres.2021.117903>, 2022.
- 864 Eilander, D.: pyFlwDir: Fast methods to work with hydro-and topography data in pure python,
865 *Zenodo [code]*, 10, 2022.
- 866 Open water quality archive datasets (WIMS): [https://environment.data.gov.uk/water-](https://environment.data.gov.uk/water-quality/view/download)
867 [quality/view/download](https://environment.data.gov.uk/water-quality/view/download), last access: 21 August 2024.
- 868 Farina, A., Di Nardo, A., Gargano, R., van der Werf, J. A., and Greco, R.: A simplified
869 approach for the hydrological simulation of urban drainage systems with SWMM, *J. Hydrol.*,
870 623, 129757, <https://doi.org/10.1016/j.jhydrol.2023.129757>, 2023.
- 871 Ghosh, I., Hellweger, F. L., and Fritch, T. G.: Fractal generation of artificial sewer networks

872 for hydrologic simulations, Proc. 2006 ESRI Int. User Conf., 1–12, 2006.

873 Gironás, J., Niemann, J. D., Roesner, L. A., Rodriguez, F., and Andrieu, H.: Evaluation of
874 Methods for Representing Urban Terrain in Storm-Water Modeling, *J. Hydrol. Eng.*, 15, 1–
875 14, [https://doi.org/10.1061/\(ASCE\)HE.1943-5584.0000142](https://doi.org/10.1061/(ASCE)HE.1943-5584.0000142), 2010.

876 Hagberg, A. A., Schult, D. A., and Swart, P. J.: Exploring Network Structure, Dynamics, and
877 Function using NetworkX, in: Proceedings of the 7th Python in Science Conference, 11–15,
878 2008.

879 Herman, J. and Usher, W.: SALib: An open-source Python library for Sensitivity Analysis, *J.*
880 *Open Source Softw.*, 2, 97, <https://doi.org/10.21105/joss.00097>, 2017.

881 Huang, Y., Zhang, J., Zheng, F., Jia, Y., Kapelan, Z., and Savic, D.: Exploring the
882 Performance of Ensemble Smoothers to Calibrate Urban Drainage Models, *Water Resour.*
883 *Res.*, 58, 1–22, <https://doi.org/10.1029/2022WR032440>, 2022.

884 Hutton, C., Wagener, T., Freer, J., Han, D., Duffy, C., and Arheimer, B.: Most computational
885 hydrology is not reproducible, so is it really science?, *Water Resour. Res.*, 52, 7548–7555,
886 <https://doi.org/10.1002/2016WR019285>, 2016.

887 Subcatchment Data Fields (InfoWorks):
888 [https://help2.innovyze.com/infoworksicm/Content/HTML/ICM_IL/Subcatchment_Data_Fields.](https://help2.innovyze.com/infoworksicm/Content/HTML/ICM_IL/Subcatchment_Data_Fields.htm)
889 [htm](https://help2.innovyze.com/infoworksicm/Content/HTML/ICM_IL/Subcatchment_Data_Fields.htm), last access: 3 June 2024.

890 Khurelbaatar, G., Al Marzuqi, B., Van Afferden, M., Müller, R. A., and Friesen, J.: Data
891 Reduced Method for Cost Comparison of Wastewater Management Scenarios–Case Study
892 for Two Settlements in Jordan and Oman, *Front. Environ. Sci.*, 9,
893 <https://doi.org/10.3389/fenvs.2021.626634>, 2021.

894 Li, X. and Willems, P.: A hybrid model for fast and probabilistic urban pluvial flood prediction,
895 *Water Resour. Res.*, 1–26, <https://doi.org/10.1029/2019wr025128>, 2020.

896 Lindsay, J. B.: Efficient hybrid breaching-filling sink removal methods for flow path
897 enforcement in digital elevation models, *Hydrol. Process.*, 30, 846–857,
898 <https://doi.org/10.1002/hyp.10648>, 2016a.

899 Lindsay, J. B.: Whitebox GAT: A case study in geomorphometric analysis., *Comput. Geosci.*,
900 95, 75–84, 2016b.

901 Mair, M., Zischg, J., Rauch, W., and Sitzenfrie, R.: Where to find water pipes and sewers?–
902 On the correlation of infrastructure networks in the urban environment, *Water (Switzerland)*,
903 9, <https://doi.org/10.3390/w9020146>, 2017.

904 McDonnell, B., Ratliff, K., Tryby, M., Wu, J., and Mullapudi, A.: PySWMM: The Python
905 Interface to Stormwater Management Model (SWMM), *J. Open Source Softw.*, 5, 2292,
906 <https://doi.org/10.21105/joss.02292>, 2020.

907 Computer generated building footprints for the United States:
908 <https://github.com/Microsoft/USBuildingFootprints?tab=readme-ov-file>, last access: 30 July
909 2024.

910 Möderl, M., Butler, D., and Rauch, W.: A stochastic approach for automatic generation of
911 urban drainage systems, *Water Sci. Technol.*, 59, 1137–1143,
912 <https://doi.org/10.2166/wst.2009.097>, 2009.

913 Möderl, M., Sitzenfrie, R., Fetz, T., Fleischhacker, E., and Rauch, W.: Systematic generation
914 of virtual networks for water supply, *Water Resour. Res.*, 47, 1–10,
915 <https://doi.org/10.1029/2009WR008951>, 2011.

916 Montalvo, C., Reyes-Silva, J. D., Sañudo, E., Cea, L., and Puertas, J.: Urban pluvial flood

- 917 modelling in the absence of sewer drainage network data: A physics-based approach, *J.*
918 *Hydrol.*, 634, 131043, <https://doi.org/10.1016/j.jhydrol.2024.131043>, 2024.
- 919 O'Callaghan, J. F. and Mark, D. M.: The extraction of drainage networks from digital
920 elevation data, *Comput. Vision, Graph. Image Process.*, 28, 323–344,
921 [https://doi.org/10.1016/S0734-189X\(84\)80011-0](https://doi.org/10.1016/S0734-189X(84)80011-0), 1984.
- 922 Ochoa-Rodriguez, S., Wang, L. P., Gires, A., Pina, R. D., Reinoso-Rondinel, R., Bruni, G.,
923 Ichiba, A., Gaitan, S., Cristiano, E., Van Assel, J., Kroll, S., Murlà-Tuyls, D., Tisserand, B.,
924 Schertzer, D., Tchiguirinskaia, I., Onof, C., Willems, P., and Ten Veldhuis, M. C.: Impact of
925 spatial and temporal resolution of rainfall inputs on urban hydrodynamic modelling outputs: A
926 multi-catchment investigation, *J. Hydrol.*, 531, 389–407,
927 <https://doi.org/10.1016/j.jhydrol.2015.05.035>, 2015.
- 928 Palmitessa, R., Grum, M., Engsig-Karup, A. P., and Löwe, R.: Accelerating hydrodynamic
929 simulations of urban drainage systems with physics-guided machine learning, *Water Res.*,
930 223, 118972, 2022.
- 931 Pedersen, A., Pedersen, J., Viguera-Rodriguez, A., Brink-Kjær, A., Borup, M., and
932 Mikkelsen, P.: The Bellinge data set: open data and models for community-wide urban
933 drainage systems research, *Earth Syst. Sci. Data Discuss.*, 13, 4779–4798,
934 <https://doi.org/10.5194/essd-2021-8>, 2021.
- 935 Pianosi, F., Beven, K., Freer, J., Hall, J. W., Rougier, J., Stephenson, D. B., and Wagener,
936 T.: Sensitivity analysis of environmental models: A systematic review with practical workflow,
937 *Environ. Model. Softw.*, 79, 214–232, <https://doi.org/10.1016/j.envsoft.2016.02.008>, 2016.
- 938 Rauch, W., Urich, C., Bach, P. M., Rogers, B. C., de Haan, F. J., Brown, R. R., Mair, M.,
939 McCarthy, D. T., Kleidorfer, M., Sitzenfrei, R., and Deletic, A.: Modelling transitions in urban
940 water systems, *Water Res.*, 126, 501–514, <https://doi.org/10.1016/j.watres.2017.09.039>,
941 2017.
- 942 Ray, G. and Sen, A.: Minimal spanning arborescence, *arXiv Prepr. arXiv2401.13238*, 2024.
- 943 Revitt, D. M., Ellis, J. B., Gilbert, N., Bryden, J., and Lundy, L.: Development and application
944 of an innovative approach to predicting pollutant concentrations in highway runoff, *Sci. Total*
945 *Environ.*, 825, 153815, 2022.
- 946 Reyes-Silva, J. D., Novoa, D., Helm, B., and Krebs, P.: An Evaluation Framework for Urban
947 Pluvial Flooding Based on Open-Access Data, *Water (Switzerland)*, 15,
948 <https://doi.org/10.3390/w15010046>, 2023.
- 949 Rossman, L. A.: Storm water management model user's manual, version 5.0, Cincinnati, 72–
950 73 pp., 2010.
- 951 Saltelli, A., Ratto, M., Andres, T., Campolongo, F., Cariboni, J., Gatelli, D., Saisana, M., and
952 Tarantola, S.: *Global Sensitivity Analysis. The Primer*, Wiley, John & Sons, 1–292 pp.,
953 <https://doi.org/10.1002/9780470725184>, 2008.
- 954 Saltelli, A., Aleksankina, K., Becker, W., Fennell, P., Ferretti, F., Holst, N., Li, S., and Wu, Q.:
955 Why so many published sensitivity analyses are false: A systematic review of sensitivity
956 analysis practices, *Environ. Model. Softw.*, 114, 29–39,
957 <https://doi.org/10.1016/j.envsoft.2019.01.012>, 2019.
- 958 Seo, Y. and Schmidt, A. R.: Network configuration and hydrograph sensitivity to storm
959 kinematics, *Water Resour. Res.*, 49, 1812–1827, <https://doi.org/10.1002/wrcr.20115>, 2013.
- 960 Sirko, W., Kashubin, S., Ritter, M., Annkah, A., Bouchareb, Y. S. E., Dauphin, Y. N.,
961 Keysers, D., Neumann, M., Cissé, M., and Quinn, J.: Continental-Scale Building Detection
962 from High Resolution Satellite Imagery, *CoRR*, abs/2107.1, 2021.

963 Sobol, I. M.: Sensitivity estimates for nonlinear mathematical models, *Math. Model. Comput.*
964 *Exp.*, 1, 407, 1993.

965 Source, M. O., McFarland, M., Emanuele, R., Morris, D., and Augspurger, T.:
966 microsoft/PlanetaryComputer: October 2022, <https://doi.org/10.5281/zenodo.7261897>,
967 October 2022.

968 Stagge, J. H., Rosenberg, D. E., Abdallah, A. M., Akbar, H., Attallah, N. A., and James, R.:
969 Assessing data availability and research reproducibility in hydrology and water resources,
970 *Sci. Data*, 6, 190030, <https://doi.org/10.1038/sdata.2019.30>, 2019.

971 Sun, S., Djordjevic, S., and Khu, S. T.: A general framework for flood risk-based storm sewer
972 network design, *Urban Water J.*, 8, 13–27, <https://doi.org/10.1080/1573062X.2010.542819>,
973 2011.

974 Sweetapple, C., Fu, G., Farmani, R., Meng, F., Ward, S., and Butler, D.: Attribute-based
975 intervention development for increasing resilience of urban drainage systems, *Water Sci.*
976 *Technol.*, 77, 1757–1764, <https://doi.org/10.2166/wst.2018.070>, 2018.

977 Sytsma, A., Crompton, O., Panos, C., Thompson, S., and Mathias Kondolf, G.: Quantifying
978 the Uncertainty Created by Non-Transferable Model Calibrations Across Climate and Land
979 Cover Scenarios: A Case Study With SWMM, *Water Resour. Res.*, 58, 1–21,
980 <https://doi.org/10.1029/2021WR031603>, 2022.

981 Tan, M. and Le, Q. V: EfficientNet: Rethinking Model Scaling for Convolutional Neural
982 Networks, *CoRR*, abs/1905.1, 2019.

983 Tarjan, R. E.: Finding optimum branchings, *Networks*, 7, 25–35,
984 <https://doi.org/10.1002/net.3230070103>, 1977.

985 Thrysoe, C., Arnbjerg-Nielsen, K., and Borup, M.: Identifying fit-for-purpose lumped
986 surrogate models for large urban drainage systems using GLUE, *J. Hydrol.*, 568, 517–533,
987 <https://doi.org/10.1016/j.jhydrol.2018.11.005>, 2019.

988 Google-Microsoft Open Buildings: [https://beta.source.coop/repositories/vida/google-](https://beta.source.coop/repositories/vida/google-microsoft-open-buildings)
989 [microsoft-open-buildings](https://beta.source.coop/repositories/vida/google-microsoft-open-buildings), last access: 30 July 2024.

990 Warsta, L., Niemi, T. J., Taka, M., Krebs, G., Haahti, K., Koivusalo, H., and Kokkonen, T.:
991 Development and application of an automated subcatchment generator for SWMM using
992 open data, *Urban Water J.*, 14, 954–963, <https://doi.org/10.1080/1573062X.2017.1325496>,
993 2017.

994 Wills, P. and Meyer, F. G.: Metrics for graph comparison: A practitioner’s guide, *PLoS One*,
995 15, e0228728, <https://doi.org/10.1371/journal.pone.0228728>, 2020.

996 Xu, Z., Dong, X., Zhao, Y., and Du, P.: Enhancing resilience of urban stormwater systems:
997 cost-effectiveness analysis of structural characteristics, *Urban Water J.*, 18, 850–859,
998 <https://doi.org/10.1080/1573062X.2021.1941139>, 2021.

999